JACS
JOURNAL OF THE AMERICAN CHEMICAL SOCIETY
Article
pubs.acs.org/JACS

Effect of Surfactant Hydrophobicity on the Pathway for Unfolding of Ubiquitin

Bryan F. Shaw,*[,†,‡,∥] Grégory F. Schneider,[†,∥] and George M. Whitesides*[,†,§]

[†]Department of Chemistry and Chemical Biology, Harvard University, Cambridge, Massachusetts 02138, United States
[‡]Department of Chemistry and Biochemistry, Baylor University, Waco, Texas, United States
[§]Wyss Institute, Harvard University, Cambridge, Massachusetts 02138, United States

Supporting Information

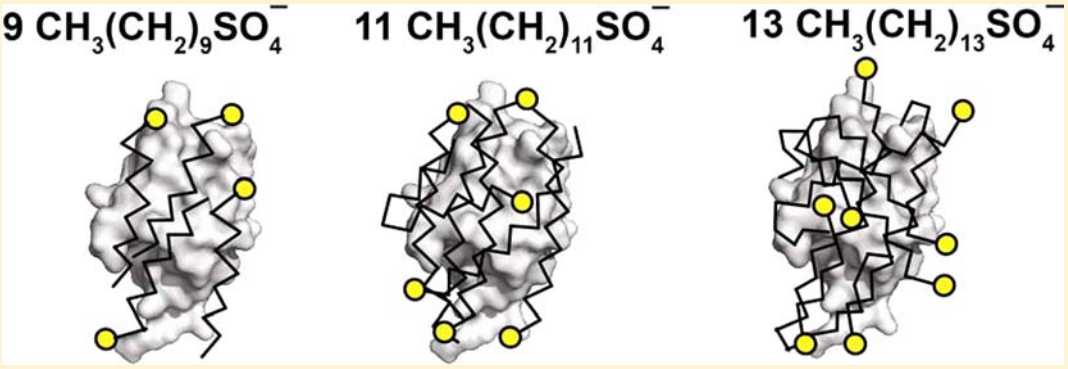

ABSTRACT: This paper describes the interaction between ubiquitin (UBI) and three sodium *n*-alkyl sulfates (SC_nS) that have the same charge ($Z = -1$) but different hydrophobicity (n = 10, 12, or 14). Increasing the hydrophobicity of the *n*-alkyl sulfate resulted in (i) an increase in the number of distinct intermediates (that is, complexes of UBI and surfactant) that form along the pathway of unfolding, (ii) a decrease in the minimum concentrations of surfactant at which intermediates begin to form (i.e., a more negative $\Delta G_{binding}$ of surfactant for UBI), and (iii) an increase in the number of surfactant molecules bound to UBI in each intermediate or complex. These results demonstrate that small changes in the hydrophobicity of a surfactant can significantly alter the binding interactions with a folded or unfolded cytosolic protein.

INTRODUCTION

Although interactions between cytosolic or non-membrane proteins and surfactants (e.g., lipids, fatty acids, or synthetic detergents) are ubiquitous in biology and biotechnology, no set of chemical principles has emerged that explains these interactions.[1−4] For example, interactions between cytosolic proteins and biological surfactants occur in many metabolic pathways,[5] in the regulation of cellular function, and in systemic physiological processes such as inflammation.[6,7] Not surprisingly, surfactant-binding proteins (e.g., fatty acid-binding proteins) represent many current drug targets for diseases that are characterized by abnormal surfactant sensing, metabolism, and accumulation,[8] including targets for obesity[5,9] and obesity-related diseases (e.g., type-II diabetes and non-alcoholic fatty liver disease, NAFLD).[10−12] The association of a cytosolic protein and surfactant can also be an early step in pathways of protein misfolding;[13−19] examples include the conversion of prion proteins (PrP^C) to toxic conformers (PrP^{SC}).

In biological systems, a cytosolic protein can interact with surfactants via (i) a transient association with a lipid membrane surface, (ii) the binding to free lipids or fatty acids, or (iii) an interaction with other molecules (drugs or metabolites) with pronounced dipolar (e.g., both hydrophobic and polar) character.[5,10,20−24]

Our recent studies of protein−surfactant interactions have established that the protein ubiquitin (UBI) and the surfactant sodium dodecyl sulfate (SDS) represent a useful model system[25] for studying both specific interactions between proteins and surfactants that do not result in a loss of protein structure and non-specific interactions above the critical micellar concentration (CMC) (which lead to unfolding).[25] We study UBI because it is (of the proteins that we have studied[26]) unique in its ability to bind multiple equivalents of SDS, below the CMC, without unfolding and to form stable, non-exchanging or slowly exchanging structures with defined stoichiometry. We chose SDS as a model surfactant for numerous technical and practical reasons: (i) SDS is highly soluble; (ii) SDS does not interfere with the spectroscopic detection of proteins at 214 nm during capillary electrophoresis (CE); (iii) the carbon chain of SDS is saturated and evenly numbered (n = 12), and near the median range of length of biological lipids and fatty acids (i.e., $4 < n < 24$);[3] and (iv) the

Received: August 10, 2012
Published: October 24, 2012

   dx.doi.org/10.1021/ja3079863 | J. Am. Chem. Soc. 2012, 134, 18739−18745

sulfate head group of SDS is similar in size to the carboxylic head group of fatty acids—and smaller than a larger lipid sphingosine or ceramide—but its permanent charge makes it electrostatically similar to anionic phosopholipids or sulfatides.[27]

We previously used CE and heteronuclear quantum coherence spectroscopy (HSQC) to define the surface properties of folded UBI that result in its simultaneous recognition of multiple molecules of SDS below the CMC.[25,28] We have also studied the pathway of unfolding of UBI in SDS above the CMC of SDS, by using CE.[25,28] Capillary electrophoresis is able to detect the binding of a single surfactant molecule to UBI, and to provide qualitative information about rates of association and dissociation. Information from CE has enabled us to identify several discrete complexes of UBI and SDS that form along the pathway of unfolding, including the thermodynamically stable complex that forms (below the CMC) between *folded* UBI and 11 equiv of SDS (i.e., UBI·$(SDS)_{11}$).

Capillary electrophoresis of UBI and peracetylated UBI in sub-micellar SDS demonstrated that cationic groups on the surface of UBI (i.e., Lys-ε-NH_3^+) are somehow fundamental in facilitating its binding to SDS below the CMC.[25] For example, the acetylation of all seven positively charged Lys-ε-NH_3^+ groups on the surface of UBI (with acetic anhydride) to yield electrostatically neutral Lys-ε-$NHCOCH_3$ groups inhibited the binding of SDS to native UBI, and prevented the formation of complexes between SDS and *native* UBI.[25] Peracetylated UBI could only bind SDS at concentrations above the CMC, where the binding coincided with the unfolding of UBI (i.e., SDS only bound peracetylated UBI in the unfolded or non-native state).

Further analysis of complexes of native UBI with multiple equivalents of SDS using HSQC NMR, and a comparison of the results with the known biophysical properties of amino acids in folded UBI (e.g., hydrophobicity, formal charge, electrostatic surface potential, secondary structure, rate of amide H/D exchange, and solvent accessibility), allowed us to identify the properties of amino acids in folded UBI that enable it to bind SDS, and to clarify how cationic groups or regions of electrostatic potential on the protein facilitate binding.[25] This previous study used $^{13}C/^{15}N-^{1}H$ HSQC to demonstrate that the binding of SDS by native UBI does not *necessarily* involve ionic interactions between R-SO_4^- and Lys-ε-NH_3^+ (although energetically important interactions do seem to occur with certain lysines). A comparison of the chemical shift perturbation ($\Delta\delta$) for each amino acid residue with its electrostatic surface potential (as calculated from solutions to the non-linear Poisson–Boltzmann equation) suggested that cationic groups in UBI facilitate the binding of SDS by contributing positive electrostatic surface potential that extends beyond the van der Waals radii of the cationic groups, into nearby hydrophobic regions that are formally neutral in charge.[25] Those hydrophobic regions in native UBI that had positive electrostatic surface potential were found to be the preferred sites of binding of SDS to UBI, as evidenced by their large values of $\Delta\delta$ during $^{15}N-^{1}H$ HSQC, or by the attenuation of signals during $^{13}C-^{1}H$ HSQC. In particular, and surprisingly (because of its low number of positively charged amino acids), the hydrophobic face of UBI that is centered around Ile44 was found to be the region that interacted most strongly with SDS. This domain is also—perhaps coincidentally—the site of binding of UBI to several hundred different proteins that possess specific types of a ubiquitin-binding domain (UBD).[29−31] This type of site—a formally neutral hydrophobic surface with a substantial surface electrostatic potential—is one that has not been included among common lists of interacting surfaces of proteins.[32,33]

The structural properties of amino acids on the surface of UBI—for example, the rate of amide H/D exchange, the solvent accessibility, and the type of secondary structure—did not appear to be factors in determining whether surface residues interacted with SDS. Residues in H-bonded loops appeared not to interact with SDS, according to HSQC.[25]

The primary objective of the current study is to determine (i) how the hydrophobicity of a surfactant affects the formation and structure of complexes between native UBI and multiple equivalents of surfactant, and (ii) how the hydrophobicity of a surfactant affects the general pathway of unfolding of UBI in solutions of surfactant, at the CMC of that surfactant and at higher concentrations. We examined the binding of a series of three sodium salts of *n*-alkyl sulfates ($C_nH_{2n+1}OSO_3^-$, n = 10, 12, or 14, abbreviated SC_nS by analogy with SDS) to folded UBI using CE. This analysis allowed us to determine how small changes in hydrophobicity of a surfactant affect the stoichiometry, affinity of surfactant binding, and pathway of unfolding (i.e., the number of intermediates that are formed along the pathway of unfolding).

The results of this study reveal a surprising number of differences among the pathways of unfolding induced by each surfactant. The results of this investigation help us to understand how folded proteins recognize *biological* surfactants.

EXPERIMENTAL DESIGN

Studying Weak Interactions between Ubiquitin and *n*-Alkyl Sulfates. We used *n*-alkyl sulfates, available in a variety of lengths (and with incrementally increasing hydrophobic surface areas), to study how hydrophobicity drives the association of surfactants and UBI. We surveyed a range of *n*-alkyl sulfates ($10 < n < 18$) but focused on just three (n = 10, 12, or 14) because each of these surfactants was highly soluble in water. This series of *n*-alkyl sulfates includes SDS and both longer and shorter surfactants, and their affinities for UBI fall in the biologically relevant range of affinities of UBDs (2 mM > K_d > 100 μM).[34]

Preparing UBI·$(SC_nS)_p$ Complexes by Dialysis. Complexes of the composition UBI·$(SC_nS)_p$ were formed by dialysis of small volumes of UBI (100 μL) against large volumes (3 L) of a solution of surfactant. Lengthy dialyses (170 h) against large volumes of surfactant produced complexes that were thermodynamic end-products for the particular concentration of free surfactant, and that were observable by CE. The concentration of unbound surfactant can be considered constant during dialysis, because the volume of the dialysis bath was so large.

Using CE To Determine How Surfactant Hydrophobicity Affects the Pathway of Denaturation of UBI and Stoichiometry of UBI–Surfactant Complexes. The analysis of UBI·$(SC_nS)_p$ with CE provides information on the number of distinct complexes, as well as the stoichiometry of these complexes. CE provides, for example, detailed information about the number and concentration of distinct complexes, and their exact stoichiometry, at a level of detail that cannot always be obtained using other methods (e.g., isothermal titration calorimetry, circular dichroism, fluorescence spectroscopy, or NMR spectroscopy).

We used CE to analyze the complexes of SC_nS surfactants with UBI after extensive dialysis (170 h), following previously published protocols.[25,28] The stoichiometry of each complex was determined with CE and protein charge ladders as previously described.[25,28] We formed charge ladders[28,35−39] of UBI by converting positively charged Lys-ε-NH_3^+ and the N-terminal α-NH_3^+ into the corresponding amides or thiocarbamoyl derivatives. The products were electrostatically neutral acetates (α- or ε-$NHCOCH_3$) or negatively charged (α-

dx.doi.org/10.1021/ja3079863 | J. Am. Chem. Soc. 2012, 134, 18739−18745

or ε-NHC═SNH-C_6H_4-SO_3^-) thiocarbamoyl sulfonate groups thereof (the phenyl group being electrostatically neutral). Each protein derivative with the same number of acetylated or thiocarbamoylated amino groups had a different net charge (Z), regardless of the location of the chemical modifications, and appeared as a distinct peak in a capillary electropherogram. The mobility of each peak of the charge ladders provided a self-calibrating tool to estimate the stoichiometry p of complexes UBI·$(SC_nS)_p$, based on a comparison of their common mobility $\mu_{UBI-(SC_nS)_p}$ with the mobilities of the rungs of the UBI charge ladder (μ_+).[38] Upon binding to UBI, each of the three n-alkyl sulfates will increase the negative charge of the resulting surfactant complex by a charge increment ΔZ (≈ 0.9, which is the charge increment in a typical acetylation charge ladder).[38] We also introduced an approximate correction for the change in mass—and thus hydrodynamic drag—that is caused by the binding of surfactant to UBI. This correction is described in the Materials and Methods section (Supporting Information).

RESULTS AND DISCUSSION

Dialysis of UBI with Free SC_nS and Analysis of UBI·$(SC_nS)_p$ Complexes Using Capillary Electrophoresis. In order to determine the specific number of complexes of UBI and surfactant that form along the unfolding pathway of UBI in SC_nS, and to determine the stoichiometry of each complex, we used CE to study the formation of the complexes UBI·$(SC_nS)_p$, formed after extensive dialysis against solutions of surfactant, at different concentrations of SC_nS.

Capillary electrophoresis confirmed the existence of multiple, distinct, thermodynamically stable (over the time for a CE experiment) complexes of UBI and SC_nS (Figure 1). These complexes have electrophoretic mobilities (μ) that range between that of native UBI (N) in the absence of surfactants (μ = 0.3 $cm^2\ kV^{-1}\ min^{-1}$; the peak for N overlaps with that of the neutral marker DMF with μ = 0 $cm^2\ kV^{-1}\ min^{-1}$) and that of denatured UBI (D) that is saturated with surfactant. Denatured UBI formed at concentrations of 50 mM for $SC_{10}S$ (μ = 20 $cm^2\ kV^{-1}\ min^{-1}$), 10 mM for $SC_{12}S$ (μ = 22 $cm^2\ kV^{-1}\ min^{-1}$), and 0.8 mM for $SC_{14}S$ (μ = 22 $cm^2\ kV^{-1}\ min^{-1}$, Figure 1).

Complexes of UBI and SC_nS surfactants could be resolved by CE into as many as seven distinct complexes, which we call N, G_1*, G_2, G_3*, G_4, G_5, and D, using a nomenclature previously described for UBI–SDS complexes.[28] We were able to estimate the number of surfactant molecules bound to UBI in each complex by comparing the electrophoretic mobility of the complex with the mobility of charge ladders of UBI. As expected, the number of molecules of SC_nS incorporated into the UBI·$(SC_nS)_p$ complexes increased with the concentration of each surfactant.

The first thermodynamically stable intermediate (G_2) that formed in each surfactant had a different number of SC_nS surfactants (ranging between 9 and 13) associated with the surface of the protein. The stoichiometry of the first stable complex (G2) was higher in solutions of $SC_{14}S$ than in solutions of $SC_{12}S$ or $SC_{10}S$ (discussed further below). Apparently, the stoichiometry of UBI–$SC_{14}S$ complexes was not reduced by the steric constraints of packing longer surfactants onto the limited surface of UBI. This observation suggests two possible characteristics for the formation of the first stable complexes of anionic surfactants with UBI: (i) that hydrophobic and electrostatic interactions operate cooperatively in causing this association between UBI and SC_nS, and/or (ii) that a surfactant that is already bound to UBI can itself interact (hydrophobically) with another surfactant in solution;

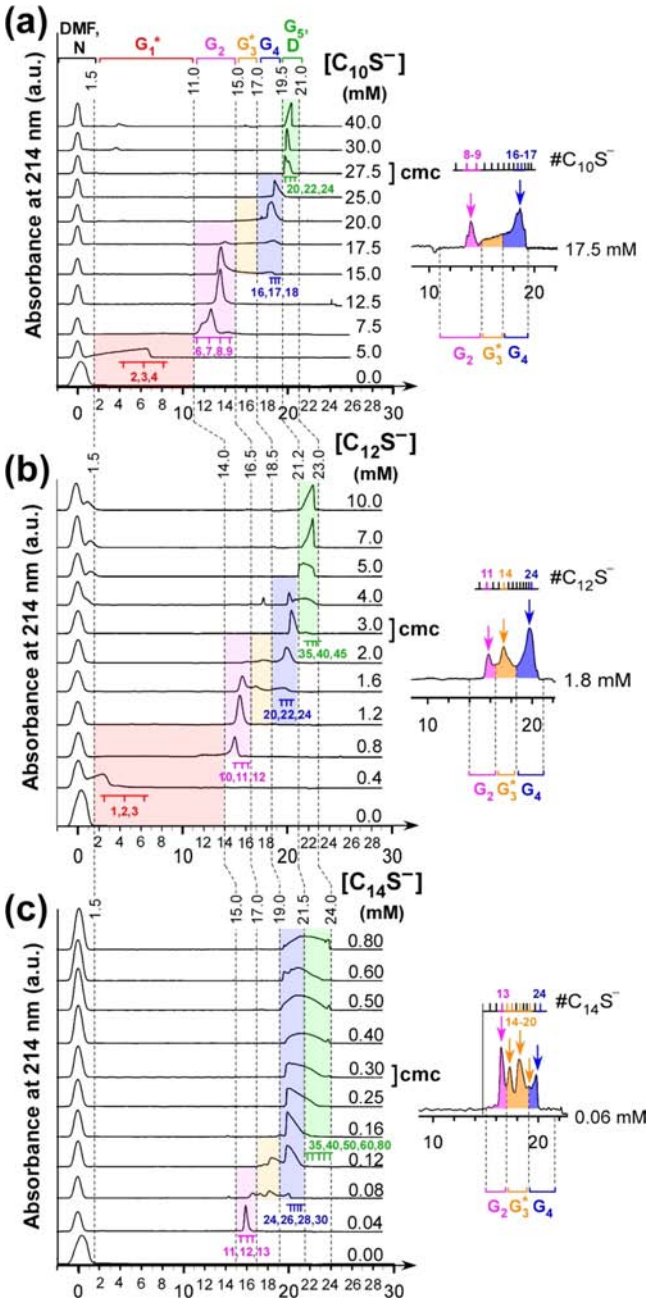

Figure 1. Electropherograms of UBI·$(SC_nS)_p$ complexes obtained after dialyzing native UBI against tris–glycine (25 mM tris, 192 mM glycine, pH 7.5, 25 °C) containing the indicated concentrations of SC_nS (from 0 to 40 mM) for 170 h. The total concentration of free UBI in the injected aliquot is [UBI] ≈ 50 μM. Each of the electropherograms is labeled with the concentration of surfactant: (a) UBI·$(SC_{10}S)_p$; (b) UBI·$(SC_{12}S)_p$; and (c) UBI·$(SC_{14}S)_p$. Colored numbers under each electropherogram designate stoichiometry (p) of surfactant molecules in UBI·$(SC_nS)_p$, as estimated from protein charge ladders. Each inset on the right-hand side of panels a–c represents an expanded electropherogram collected at a specific concentration of surfactant that resulted in multiple unique UBI·$(SC_nS)_p$ complexes (denoted G_2, G_3, and G_4) that formed below the CMC; colored numbers on top of each electropherogram (labeled "#C_nS^-") designate surfactant stoichiometry. The electrically neutral marker is DMF (used to calibrate the rate of electro-osmotic flow in the experiment); the neutral marker overlaps with the native (N) UBI in the absence of surfactant. The critical micelle concentration of surfactant is highlighted with a bracket labeled "CMC" and was inferred from the appearance of complexes of UBI and SC_nS within the

dx.doi.org/10.1021/ja3079863 | J. Am. Chem. Soc. 2012, 134, 18739–18745

Figure 1. continued

group G_5. Dotted vertical lines represent electrophoretic boundaries where each group (G) of UBI·$(SC_nS)_p$ complexes forms (including N and D). The *y* axes are in arbitrary units of absorbance (a.u.), that is, the reading of the CE trace; the *x* axes are in units of mobility (cm^2 kV^{-1} min^{-1}). The total integrated area due to protein should be approximately consistent in each experiment.

i.e., that surfactant that is bound to SDS can nucleate the condensation of additional surfactant via hydrophobic interactions.

Using Charge Ladders and CE To Quantify the Stoichiometry of UBI·$(SC_nS)_p$ Complexes. We used protein charge ladders of UBI to approximate the exact stoichiometry of the UBI·$(SC_nS)_p$ complexes by comparing the mobilities of UBI·$(SC_nS)_p$ complexes with rungs of a charge ladder of UBI (Figures 1 and 2). We assumed for this analysis that the charge

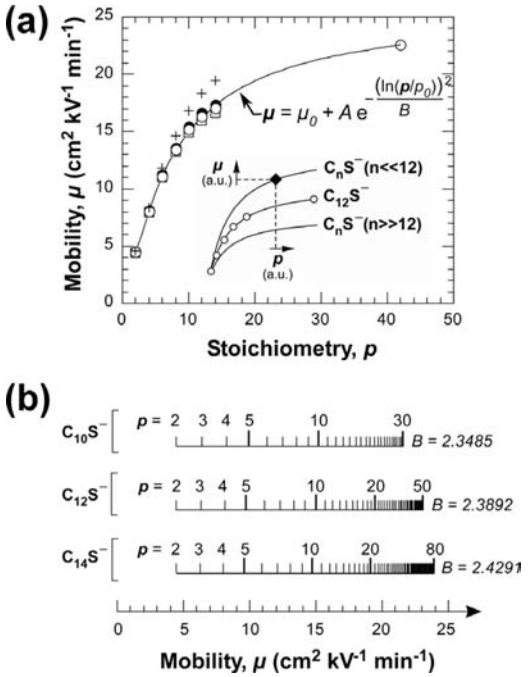

Figure 2. Stoichiometry of UBI–detergent complexes. (a) Stoichiometry *p* of UBI·$(SC_nS)_p$ complexes was estimated using 4-sulfophenylisothiocyanate charge ladders of UBI (refer to ref 23 for original electropherograms of the charge ladder). Experimental mobilities of rungs of a 4-sulfophenylisothiocyanate charge ladders of UBI (denoted by "+" curve), and mobilities after their calibration (i.e., correction) using eq 2 displayed in the Supporting Information: (●) for $SC_{10}S$, (○) for $SC_{12}S$, and (□) for $SC_{14}S$. Schematic inset shows how plot of μ vs *p* will shift as hydrophobicity of surfactant increases or decreases. (b) Stoichiometry ruler for each surfactant (derived from panel a) illustrating difference in mobility of each UBI·$(SC_nS)_p$ complex and the observed range of stoichiometry of complexes of UBI·$(SC_nS)_p$.

regulation in UBI·$(SC_nS)_p$ complexes that probably occurs upon the binding of SC_nS to UBI is equal to that resulting from the acetylation of lysines in a charge ladder of UBI.[39] We also corrected for the increased molecular weight and hydrodynamic drag resulting from the binding of surfactant molecules. For analytical details see the Experimental Design section.

Protein charge ladders can only be used to directly approximate the stoichiometry (i.e., mobilitiy) of UBI·$(SC_nS)_p$ complexes that have low stoichiometry (i.e., $p < 16$ SC_nS molecules). In order to estimate the stoichiometry of UBI·$(SC_nS)_p$ complexes with higher stoichiometry (i.e., $p >$ 16 SC_nS molecules), the plot of mobility versus the number of acylated residues for the charge ladder (Figure 2a) must be mathematically extrapolated. For example, there are only seven Lys-ε-NH_3^+ groups in UBI (and one N-terminal α-NH_3^+); the thiocarbamoylation of each R-NH_3^+ to R-NHC═SNH-C_6H_4-SO_3^- is electrostatically equivalent (approximately) to the binding of *two* molecules of SC_nS. The R-NHC═SNH-C_6H_4–SO_3^- charge ladder can, therefore, estimate the stoichiometry of UBI·$(SC_nS)_p$ complexes with $p < 16$ molecules of surfactant.

The values of electrophoretic mobilities that define a specific group of complexes (e.g., G_2) increased as the hydrophobicity of the surfactant increased (mobilities are listed over each electropherogram in Figure 1). The higher mobility of complexes with surfactants with longer *n*-alkyl tails (e.g., $SC_{12}S$, $SC_{14}S$) suggests that these complexes contain greater numbers of surfactants than analogous complexes of UBI·$(SC_{10}S)_p$.

Hydrophobicity of SC_nS Affects the Stoichiometry of Thermodynamically Stable Complexes G_2, G_4, and D. Capillary electrophoresis demonstrated that UBI forms a specific G_2 complex (i.e., UBI·$(SC_nS)_p$) with each surfactant. The concentration of surfactant at which each G_2 complex forms (which we refer to as the "critical complex concentration") decreases as the surfactant hydrophobicity increases. The stoichiometry of each G_2 complex (*p*) increased with the length of the chain of the SC_nS species. For example, for $SC_{10}S$, $p = 9$; for $SC_{12}S$, $p = 11$; for $SC_{14}S$, $p = 13$. The complexes between UBI and each of the three surfactants that formed near or above the CMC probably include UBI in a non-native structure; these complexes (i.e., G_4 and D) had greater differences in stoichiometry than the complexes such as G_2 that formed far below the CMC (and probably consist of natively folded UBI). This point is demonstrated by the increasing slopes of the three regression lines of *p* vs *n*: ~1.0 for G_2, ~2.5 for G_4, and ~9.2 for D (Figure 3b). The difference between these slopes suggests that hydrophobic interactions between UBI and *n*-alkyl sulfates become stronger at higher concentrations of surfactant, and greater hydrophobicity of surfactant. The stable intermediates G_4 and D, which formed at higher concentration of surfactants than G_2, are, therefore, capable of binding a greater number of longer surfactant (i.e., C_{14}) than shorter surfactant (i.e., C_{10}). This trend toward larger aggregation numbers for longer surfactants is not surprising (in this particular system) when considering that hydrophobic interactions seem to be the major driving force in binding of surfactants to UBI at high concentrations of surfactant (>CMC).[40] The positive correlation between aggregation number and hydrophobicity is not necessarily a general effect: in systems other than UBI and alkyl sulfates—for example, in systems where surfactants of different hydrophobicity might have similar binding constants—one might expect that higher aggregation numbers would be observed for smaller alkyl chains, because a greater number of molecules is required to cover the surface of the protein.

Our previous HSQC study demonstrated that the binding of 11 SDS to native UBI caused substantial changes in the $\Delta\delta$'s of residues throughout this protein. The greatest perturbations were, however, seen in residues at the hydrophobic patch that centers around Ile44. This patch—which is on the positively charged face of the electrostatically Janus-faced UBI—is the

dx.doi.org/10.1021/ja3079863 | J. Am. Chem. Soc. 2012, 134, 18739–18745

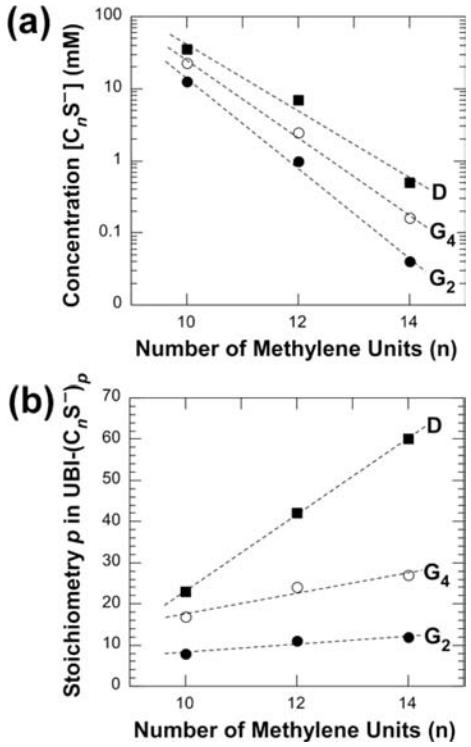

Figure 3. Dependence of the stoichiometry of UBI–surfactant complexes, and the critical complex concentration, on the number of methylene groups of surfactant. (a) Plot of the critical complex concentration (denoted CCC) of SC_nS surfactant (i.e., concentration of surfactant at which G_2, G_4, and D complexes formed) as a function of the number of methylene units in each surfactant. The CCC of the G_2, G_4, and D UBI–surfactant complexes decreased with increasing hydrophobicity of the surfactant. (b) Plot of the stoichiometry p in UBI·$(SC_nS)_p$ complexes G_2, G_4, and D as a function of the number of methylene units in each surfactant. The stoichiometry of each UBI·$(SC_nS)_p$ complex increases with the hydrophobicity of the surfactant.

binding site for many different polypeptides that possess UBDs.[29–31] The results of this study and our previous study suggest that multiple surfactants bind to the hydrophobic Ile44 region of UBI. We do not assume, however, that *all* 13 $SC_{13}S$ molecules in the G_2 complex, for example, bind at the Ile44 hydrophobic face. The surface area of this hydrophobic patch of UBI is simply not large enough to accommodate 13 molecules of $SC_{14}S$ (unless the surfactants were undergoing hydrophobic interactions with one another that facilitated their stacking upon the Ile44 patch, outward to solvent—which we cannot exclude).

In summary, we estimated that each pair of additional methylene units in the series of *n*-alkyl sulfates (i.e., n = 10, 12, or 14) resulted in the additional binding of approximately two surfactant molecules in the transition from N to G_2; about five surfactant molecules in the transition from N to G_4; and approximately 18 surfactant molecules in the transition from N to D (Figure 3a). The effect of increasing the hydrophobicity of the surfactant on the stoichiometry of the UBI·$(SC_nS)_p$ complexes is therefore cumulative, and larger for later (G_4 and D) than earlier intermediates (G_2) along the pathway to complete denaturation and saturating interaction with surfactant.

Hydrophobicity of SC_nS Affects the Number of Observable Complexes with Distinct Electrophoretic Mobilities. An increase in the length of the *n*-alkyl sulfate increases the number of different protein–surfactant complexes that form after G_2. For example, the transition from G_2 to G_4 that occurs during the binding of $SC_{10}S$ is characterized by a single broad peak (see group labeled G_3* in the three right insets in Figure 1); the G_2-to-G_4 transition that occurs during the binding of $SC_{12}S$ is characterized by two resolvable peaks; the G_2-to-G_4 transition in $SC_{14}S$ yielded three resolvable peaks (that is, one or two G_3* complexes could be resolved in the presence of $SC_{12}S$ or $SC_{14}S$, but not $SC_{10}S$). The observed reduction in the width for peaks of G_3* in the presence of longer surfactants is consistent with a greater stability of complexes with intermediate stoichiometry for longer *n*-alkyl sulfates, such as UBI·$(SC_{14}S)_{14}$ and UBI·$(SC_{14}S)_{20}$.

The increase in the number of G_3* complexes with distinct mobilities between G_2 and G_4 as the surfactant hydrophobicity increases suggests that (i) different complexes are forming (with unique stoichiometry) as a result of different modes of binding of UBI, or (ii) the binding of additional molecules of surfactant is energetically unfavorable because, for example, a re-arrangement of previously bound molecules must occur before the binding of additional surfactant. Despite the differences in stoichiometry of these intermediate G_3* complexes, each must be thermodynamically stable; otherwise, it would revert to G_2 via desorption of bound surfactants, or would produce a peak with intermediate mobility (as appears to be the case with $SC_{10}S$, see inset in Figure 1a).

The complexes of G_5 and D that formed upon the binding of $SC_{10}S$ or $SC_{12}S$ were separable by CE. The G_5 and D complexes that formed in $SC_{14}S$, however, were not resolved by CE. The peak corresponding to the G_5 intermediate is broader in $SC_{14}S$ than in shorter surfactants (Figure 1). We suggest that the low resolution of G_5 and D in $SC_{14}S$ is caused by the increased heterogeneity of complexes (e.g., "mixed protein–surfactant micelles" [38,41]).

Using CE To Estimate the Free Energies of Binding of Anionic Surfactants to UBI in Saturated (Dialyzed) Complexes. We can use CE to estimate the average affinity of binding of surfactants to UBI on the basis of the concentration of surfactant at which each different complex formed (i.e., the "CCC"). This concentration of surfactant influences the distribution of protein–surfactant complex species within each group (N, G_1*, G_2, G_3*, G_4, G_5, G_6*, and D), as would be anticipated if hydrophobic interaction were important in determination of pathways of interaction of surfactants with proteins. Increasing the length of the alkyl chain of the surfactant decreases the equilibrium concentration of surfactant required to form complexes within a specific group. For example, dialyzed samples of UBI (50 μM) formed G_2 intermediate at concentrations [$SC_{10}S$] = 12.5 mM, at [$SC_{12}S$] = 1.2 mM, and at [$SC_{14}S$] = 0.04 mM, Figure 1. The equilibrium concentration of surfactant required to form G_2 is reduced by a factor of 10–30 (corresponding to a difference in free energy of $\Delta\Delta G^\circ \approx$ 1.3–1.6 kcal/mol) for each pair of additional methylene units added to the hydrophobic tail of the surfactant in the series. This value of $\Delta\Delta G^\circ$ corresponds to −21.4 cal mol^{-1} Å^{-2} energy of burying a hydrophobic surface (assuming the entire surface is buried). This value is somewhat higher than the reported value of −15 cal mol^{-1} Å^{-2} associated with variation of hydrophobic interface between protein subunits,[42] but lower than −30 cal mol^{-1} Å^{-2} for burying hydrophobic surface due to the ordering of water molecules.[43,44] The calculated $\Delta\Delta G^\circ$ of interactions of excess of

dx.doi.org/10.1021/ja3079863 | J. Am. Chem. Soc. 2012, 134, 18739–18745

SC_nS surfactants with UBI thus lies within the expected range of energies for burying hydrophobic surface of proteins.

CONCLUSIONS

We have studied interactions of ubiquitin with *n*-alkyl sulfates (n = 10, 12, or 14). An increase in the hydrophobicity of an *n*-alkyl sulfate affected several properties of UBI·$(SC_nS)_p$ complexes. In particular, increasing the hydrophobicity of an *n*-alkyl sulfate resulted in (i) an increase in the affinity of surfactants for UBI, (ii) an increase in the number of distinct complexes of UBI·$(SC_nS)_p$, and (iii) an increase in the stoichiometric ratio of surfactant to UBI in each native or denatured complex. These increases were semi-quantitatively in line with expectations for increasing areas of interacting hydrophobic surfaces.

The interactions between proteins and surfactants have been historically difficult to study because the surfaces of most proteins are chemically heterogeneous and structurally dynamic (i.e., each conformation within a native ensemble[45−47] or denatured ensemble[48,49] contains multiple types of functional groups positioned in different configurations). We believe that it will be possible to infer greater detail concerning the interactions of proteins and surfactants than we have achieved with UBI in this study and our two previous studies[25,28] by limiting further the complexity of the problem via the study of smaller proteins. The Trp-cage protein (PDB: 1L2Y), for example, is one of the smallest folded proteins found in living systems.[50,51] This 20-residue-long protein (derived from the saliva of Gila monsters) consists of three turns of an α-helix and a single flexible loop; its structure and pathway of folding have been studied extensively.[52−61] Identifying (or engineering) a small folded protein, similar to Trp-cage protein, that could bind SDS below the CMC, and then systematically substituting amino acids via mutagenesis, would further clarify how details of the surface chemistry of a folded protein (e.g., aromaticity—a property that we have not studied) might facilitate the self-assembly of multiple surfactants onto that surface.

ASSOCIATED CONTENT

Supporting Information

Additional experimental details. This material is available free of charge via the Internet at http://pubs.acs.org.

AUTHOR INFORMATION

Corresponding Author

bryan_shaw@baylor.edu; gwhitesides@gmwgroup.harvard.edu

Author Contributions

‖B.F.S. and G.F.S. contributed equally.

Notes

The authors declare no competing financial interest.

ACKNOWLEDGMENTS

This research was funded by NIH award GM 051559. B.F.S. was supported by a NIH Ruth L. Kirchstein NRSA post-doctoral fellowship (GM081055) and by a startup fund from Baylor University. G.F.S. was supported by a "Lavoisier Générale" post-doctoral fellowship (Ministère des Affaires Etrangères Français).

REFERENCES

(1) Fu, L.; Liu, J.; Yan, E. C. *J. Am. Chem. Soc.* **2011**, *133*, 8094.
(2) Best, M. D.; Rowland, M. M.; Bostic, H. E. *Acc. Chem. Res.* **2011**, *44*, 686.
(3) Shi, Y.; Mowery, R. A.; Ashley, J.; Hentz, M.; Ramirez, A. J.; Bilgicer, B.; Slunt-Brown, H.; Borchelt, D. R.; Shaw, B. F. *Protein Sci.* **2012**, *21*, 1197.
(4) Otzen, D. *Biochim. Biophys. Acta* **2011**, *1814*, 562.
(5) Ichimura, A.; et al. *Nature* **2012**, *483*, 350.
(6) Yamamoto, K.; Isogai, Y.; Sato, H.; Taketomi, Y.; Murakami, M. *Anal. Bioanal. Chem.* **2011**, *400*, 1829.
(7) Liao, W. L.; Wang, W. C.; Chang, W. C.; Tseng, J. T. *J. Biol. Chem.* **2011**, *286*, 35499.
(8) Koutsari, C.; Mundi, M. S.; Ali, A. H.; Jensen, M. D. *Diabetes* **2012**, *61*, 329.
(9) Powell, A. G.; Apovian, C. M.; Aronne, L. J. *Clin. Pharmacol. Ther.* **2011**, *90*, 40.
(10) Braca, A.; Dal Piaz, F.; Marzocco, S.; Autore, G.; Vassallo, A.; De Tommasi, N. *Curr. Drug Targets* **2011**, *12*, 302.
(11) Shirfule, A. L.; Sangamwar, A. T.; Khobragade, C. N. *Int. J. Biol. Macromol.* **2011**, *49*, 62.
(12) Martinez-Clemente, M.; Claria, J.; Titos, E. *Curr. Opin. Clin. Nutr. Metab. Care* **2011**, *14*, 347.
(13) Wang, F.; Yin, S.; Wang, X.; Zha, L.; Sy, M. S.; Ma, J. *Biochemistry* **2010**, *49*, 8169.
(14) Beel, A. J.; Sakakura, M.; Barrett, P. J.; Sanders, C. R. *Biochim. Biophys. Acta* **2010**, *1801*, 975.
(15) Chich, J. F.; Chapuis, C.; Henry, C.; Vidic, J.; Rezaei, H.; Noinville, S. *J. Mol. Biol.* **2010**, *397*, 1017.
(16) Shvadchak, V. V.; Yushchenko, D. A.; Pievo, R.; Jovin, T. M. *FEBS Lett.* **2011**, *585*, 3513.
(17) Ryan, T. M.; Griffin, M. D.; Teoh, C. L.; Ooi, J.; Howlett, G. J. *J. Mol. Biol.* **2011**, *406*, 416.
(18) Choi, I.; Yang, Y. I.; Song, H. D.; Lee, J. S.; Kang, T.; Sung, J. J.; Yi, J. *Biochim. Biophys. Acta* **2011**, *1812*, 41.
(19) Bartels, T.; Choi, J. G.; Selkoe, D. J. *Nature* **2011**, *477*, 107.
(20) Min, Y.; Kristiansen, K.; Boggs, J. M.; Husted, C.; Zasadzinski, J. A.; Israelachvili, J. *Proc. Natl. Acad. Sci. U.S.A.* **2009**, *106*, 3154.
(21) Ji, S. R.; Ma, L.; Bai, C. J.; Shi, J. M.; Li, H. Y.; Potempa, L. A.; Filep, J. G.; Zhao, J.; Wu, Y. *FASEB J.* **2009**, *23*, 1806.
(22) Jenkins, R. W.; Idkowiak-Baldys, J.; Simbari, F.; Canals, D.; Roddy, P.; Riner, C. D.; Clarke, C. J.; Hannun, Y. A. *J. Biol. Chem.* **2011**, *286*, 3777.
(23) Wu, B. X.; Clarke, C. J.; Matmati, N.; Montefusco, D.; Bartke, N.; Hannun, Y. A. *J. Biol. Chem.* **2011**, *286*, 22362.
(24) Miyauchi, S.; Hirasawa, A.; Ichimura, A.; Hara, T.; Tsujimoto, G. *J. Pharm. Sci.* **2010**, *112*, 19.
(25) Shaw, B. F.; Schneider, G. F.; Arthanari, H.; Narovlyansky, M.; Moustakas, D.; Durazo, A.; Wagner, G.; Whitesides, G. M. *J. Am. Chem. Soc.* **2011**, *133*, 17681.
(26) Gudiksen, K. L.; Gitlin, I.; Whitesides, G. M. *Proc. Natl. Acad. Sci. U.S.A.* **2006**, *103*, 7968.
(27) Takahashi, T.; Suzuki, T. *J. Lipid Res.* **2012**, *53*, 1437.
(28) Schneider, G. F.; Shaw, B. F.; Lee, A.; Carillho, E.; Whitesides, G. M. *J. Am. Chem. Soc.* **2008**, *130*, 17384.
(29) Grabbe, C.; Dikic, I. *Chem. Rev.* **2009**, *109*, 1481.
(30) Kim, H. C.; Steffen, A. M.; Oldham, M. L.; Chen, J.; Huibregtse, J. M. *EMBO Rep.* **2011**, *12*, 334.
(31) Pinato, S.; Gatti, M.; Scandiuzzi, C.; Confalonieri, S.; Penengo, L. *Mol. Cell. Biol.* **2011**, *31*, 118.
(32) Hudson, B. D.; Tikhonova, I. G.; Pandey, S. K.; Ulven, T.; Milligan, G. *J. Biol. Chem.* **2012**, in press.
(33) Schneider, S.; Zacharias, M. *J. Struct. Biol.* **2012**, in press.
(34) Hurley, J. H. L., S.; Prag, G. *Biochem. J.* **2006**, *399*, 361.
(35) Colton, I. J.; Anderson, J. R.; Gao, J. M.; Chapman, R. G.; Isaacs, L.; Whitesides, G. M. *J. Am. Chem. Soc.* **1997**, *119*, 12701.
(36) Gao, J. M.; Gomez, F. A.; Harter, R.; Whitesides, G. M. *Proc. Natl. Acad. Sci. U.S.A.* **1994**, *91*, 12027.
(37) Gao, J. M.; Mammen, M.; Whitesides, G. M. *Science* **1996**, *272*, 535.

(38) Gitlin, I.; Carbeck, J. D.; Whitesides, G. M. *Angew. Chem., Int. Ed.* **2006**, *45*, 3022.
(39) Gitlin, I.; Mayer, M.; Whitesides, G. M. *J. Phys. Chem. B* **2003**, *107*, 1466.
(40) Haldar, B. C., A.; Mallick, A.; Mandal, M. C.; Das, P.; Chattopadhyay, N. *Langmuir* **2006**, *22*, 3514.
(41) Gudiksen, K. L.; Gitlin, I.; Moustakas, D. T.; Whitesides, G. M. *Biophys. J.* **2006**, *91*, 298.
(42) Vallone, B. M.; Adriana, E.; Vecchini, P.; Chiancone, E.; Brunori, M. *Proc. Natl. Acad. Sci. USA.* **1998**, *95*, 6103.
(43) Wermuth, C. G. *The Practice of Medicinal Chemistry*, 3rd ed.; Academic Press: New York, 2008.
(44) Snyder, P. W.; Mecinovic, J.; Moustakas, D. T.; Thomas, S. W., III; Harder, M.; Mack, E. T.; Lockett, M. R.; Heroux, A.; Sherman, W.; Whitesides, G. M. *Proc. Natl. Acad. Sci. U.S.A.* **2011**, *108*, 17889.
(45) Naganathan, A. N.; Orozco, M. *J. Am. Chem. Soc.* **2011**, *133*, 12154.
(46) Ayuso-Tejedor, S.; Garcia-Fandino, R.; Orozco, M.; Sancho, J.; Bernado, P. *J. Mol. Biol.* **2011**, *406*, 604.
(47) Chandra, K.; Sharma, Y.; Chary, K. V. *Biochim. Biophys. Acta* **2011**, *1814*, 334.
(48) Meng, W.; Raleigh, D. P. *Proteins* **2011**, *79*, 3500.
(49) Dar, T. A.; Schaeffer, R. D.; Daggett, V.; Bowler, B. E. *Biochemistry* **2011**, *50*, 1029.
(50) Paschek, D.; Day, R.; Garcia, A. E. *Phys. Chem. Chem. Phys.* **2011**, *13*, 19840.
(51) Jimenez-Cruz, C. A.; Makhatadze, G. I.; Garcia, A. E. *Phys. Chem. Chem. Phys.* **2011**, *13*, 17056.
(52) Vymetal, J.; Vondrasek, J. *J. Phys. Chem. A* **2011**, *115*, 11455.
(53) Culik, R. M.; Serrano, A. L.; Bunagan, M. R.; Gai, F. *Angew. Chem., Int. Ed.* **2011**, *50*, 10884.
(54) Heyda, J.; Kozisek, M.; Bednarova, L.; Thompson, G.; Konvalinka, J.; Vondrasek, J.; Jungwirth, P. *J. Phys. Chem. B* **2011**, *115*, 8910.
(55) Velez-Vega, C.; Borrero, E. E.; Escobedo, F. A. *J. Chem. Phys.* **2010**, *133*, 105103.
(56) Day, R.; Paschek, D.; Garcia, A. E. *Proteins* **2010**, *78*, 1889.
(57) Wafer, L. N.; Streicher, W. W.; Makhatadze, G. I. *Proteins* **2010**, *78*, 1376.
(58) Gattin, Z.; Riniker, S.; Hore, P. J.; Mok, K. H.; van Gunsteren, W. F. *Protein Sci.* **2009**, *18*, 2090.
(59) Marinelli, F.; Pietrucci, F.; Laio, A.; Piana, S. *PLoS Comput. Biol.* **2009**, *5*, e1000452.
(60) Cerny, J.; Vondrasek, J.; Hobza, P. *J. Phys. Chem. B* **2009**, *113*, 5657.
(61) Ding, F.; Buldyrev, S. V.; Dokholyan, N. V. *Biophys. J.* **2005**, *88*, 147.